Food Chemistry: Molecular Sciences 7 (2023) 100176

Contents lists available at ScienceDirect

Food Chemistry: Molecular Sciences

journal homepage: www.sciencedirect.com/journal/food-chemistry-molecular-sciences

Comprehensive analysis of transcriptome and metabolome provides insights into the stress response mechanisms of apple fruit to postharvest impact damage

Zhichao Yang [a], Menghua Lin [b], Xiangzheng Yang [b,d], Di Wu [a,b,c,*], Kunsong Chen [b]

[a] College of Biosystems Engineering and Food Science, Zhejiang University, Hangzhou 310058, PR China
[b] College of Agriculture & Biotechnology/Zhejiang Provincial Key Laboratory of Horticultural Plant Integrative Biology/The State Agriculture Ministry Laboratory of Horticultural Plant Growth, Development and Quality Improvement, Zhejiang University, Zijingang Campus, Hangzhou 310058, PR China
[c] Zhejiang University Zhongyuan Institute, Zhengzhou 450000, PR China
[d] Jinan Fruit Research Institute, All China Federation of Supply and Marketing Cooperatives, Jinan 250014, PR China

ARTICLE INFO

Keywords:
Transcriptome
Metabolome
Apple fruit
Impact damage
Resistance mechanisms

ABSTRACT

An integrated analysis of the transcriptome and metabolome was conducted to investigate the underlying mechanisms of apple fruit response to impact damage stress. During the post-damage storage, a total of 124 differentially expressed genes (DEGs) were identified, which were mainly annotated in 13 pathways, including phenylpropanoid biosynthesis. Besides, 175 differentially expressed metabolites (DEMs), including 142 up-regulated and 33 down-regulated metabolites, exhibited significant alteration after impact damage. The DEGs and DEMs were simultaneously annotated in 7 metabolic pathways, including flavonoid biosynthesis. Key genes in the volatile esters and flavonoid biosynthesis pathways were revealed, which may play a crucial role in the coping mechanisms of apple fruit under impact damage stress. Moreover, 13 ABC transporters were significantly upregulated, indicating that ABC transporters may contribute to the transportation of secondary metabolites associated with response to impact damage stress. The results may elucidate the comprehension of metabolic networks and molecular mechanisms in apple fruits that have undergone impact damage.

1. Introduction

The hybrid analysis of multiple omics, such as genomics, transcriptomics, proteomics, and metabolomics, constitutes a crucial strategy for investigating the interactions among distinct substances in biological systems (Afridi et al., 2022; Pinu et al., 2019; Zheng et al., 2022). As multi-omics analysis methods continue to advance, an escalating number of inquiries employ transcriptomics and metabolomics to elucidate the underlying mechanisms governing fruit responses to non-biological stress (J. Liu et al., 2022). For instance, Yun et al. (2016) utilized transcriptomics and metabolomics to scrutinize the regulatory mechanism of hastened senescence in Litchi fruit following cold storage. Their findings indicated that rapid aging of Litchi fruit after cold storage might be due to oxidative processes induced by abscisic acid, which included the oxidation of lipids, polyphenols, and anthocyanins. Similarly, Lin et al. (2021) conducted a transcriptomic and metabolomic analysis of *Lycium barbarum* fruit under salt stress, thereby identifying 1396 genes with differential expression and 71 metabolites with differential expression. The pathway analysis conducted revealed that the flavonoid metabolism pathway could heighten the salt tolerance of *Lycium barbarum* fruit. However, scant reports are available on the use of transcriptomics and metabolomics to probe the response mechanisms of fruits to postharvest mechanical damage stress.

Transcriptomics is a valuable technique for investigating gene expression and transcriptional regulation at the mRNA level, which allows researchers to probe cellular phenotypes and functions (X. Liu et al., 2023; M. Zhang et al., 2022). This method has found extensive use in various postharvest fruit research fields, including investigations into molecular mechanisms under non-biological stress. For example, Gong et al. (2015) observed that differentially expressed genes linked to brassinosteroid biosynthesis and the phosphatidylinositol signaling system were upregulated in loquat fruits subjected to cold stress, highlighting their critical role in the fruit's resistance mechanism against cold stress. Similarly, Zhang et al. (2020) found that cold-stressed

* Corresponding author at: College of Agriculture & Biotechnology, Zhejiang University, Hangzhou 310058, PR China.
E-mail address: di_wu@zju.edu.cn (D. Wu).

https://doi.org/10.1016/j.fochms.2023.100176
Received 31 March 2023; Received in revised form 6 June 2023; Accepted 1 July 2023
Available online 3 July 2023

blueberry fruits primarily induced genes involved in the biosynthesis of membrane lipids, proline, glutathione, flavonoids, brassinosteroids, carotenoids, and zeatin. Meanwhile, Belay et al. (2020) found that differentially expressed genes related to cell membrane proteins, glycine-rich proteins, glycosyltransferase proteins, and tannin biosynthesis were mainly associated with the "scald" injury in pomegranate peel during low-temperature storage.

Metabolomics represents a burgeoning field that has emerged in the wake of genomics, transcriptomics, and proteomics, and is a pivotal constituent of systems biology. The examination of metabolomics is of paramount importance in scrutinizing non-biological stress response mechanisms in fruits (Shen et al., 2021). A comparative analysis of metabolomic data conducted by Moreno et al. (2018) on two citrus cultivars, 'Murcott' and 'Ellendale', revealed that 'Ellendale' evinced a robust capacity to withstand both biological and non-biological stress following heat treatment. In a study by Tunsagool et al. (2019), it was demonstrated that the application of *Bacillus subtilis* lipopeptides could mediate citrus fruit's resistance response to stress. The application of lipopeptides upregulated the levels of serotonin and tyramine, two important secondary metabolites that have been reported to stimulate the plant defense system during stress. Furthermore, metabolic pathway analysis revealed that the application of *Bacillus subtilis* lipopeptides triggers the metabolism of glycine, serine, and threonine, which are the primary pathways inducing serotonin production, and activates tyrosine metabolism, leading to an increase in tyramine production. Santin et al. (2021) discovered that UV-B stress had a considerable influence on the metabolome of peach fruits. Specifically, terpenes, phenylpropanoids, plant toxins, and fatty acids decreased in content after 24 h of UV-B treatment, but increased after 36 h.

Mechanical damage represents a recurrent and pervasive issue in fruit cultivation and preservation, which can culminate in notable financial deficits for growers, manufacturers, and vendors. Such impairment can elicit physical and physiological alterations in fruit tissues, instigating a reduction in firmness, an escalation in respiration rates, and an amplification in the predisposition towards putrefaction and microbial contamination, thereby expediting the proliferation of deteriorated fruit, curtailing fruit shelf-life, and ultimately incurring substantial economic losses for agricultural production (Lin et al., 2021). Among the various modalities of mechanical damage, impact damage, resulting from dynamic loading, constitutes a predominant form of post-harvest fruit impairment (Lin et al., 2022). This damage typically occurs during rough handling in fruit loading and unloading, commercial processing, grading and sorting, as well as collisions with conveyors during transportation or as a result of packaging falling or sudden braking.

Most of the fruit species including apple are gained more popularity in recently and the number of scientific studies on fruit species has been increased. These fruits are genetically very diverse and among the healthiest foods and provide a number of impressive health benefits. They include high content of non-nutritive, nutritive, and bioactive compounds such as flavonoids, phenolics, anthocyanins, phenolic acids, and as well as nutritive compounds such as sugars, essential oils, carotenoids, vitamins, and minerals (Abanoz & Okcu, 2022; Bozhuyuk, 2022; Dawadi et al., 2022; Rymbai et al., 2023). The 'Red Fuji' apple (*Malus* × *domestica Borkh*. Red Fuji) is a widely recognized fruit belonging to the Rosaceae family. Nonetheless, its delicate skin and fragile texture render it vulnerable to damage during the post-harvest supply chain, which could result in decay and deterioration (Lin et al., 2021). Although some preliminary investigations have been conducted on the molecular mechanisms underpinning the deterioration of apple fruit quality and stress response triggered by post-harvest mechanical damage, there exists a dearth of systematic research on the stress response mechanisms of apple fruit subjected to impact damage, as well as the metabolic network and molecular mechanisms of physiological deterioration induced by impact damage.

The present investigation entailed a comprehensive analysis of the stress response mechanism of 'Red Fuji' apple fruit subjected to impact damage, utilizing an integrated approach involving transcriptomic and metabolomic analyses. The screening of candidate defense compounds and genes, alongside the clarification of the metabolic regulation network under impact damage stress, were accomplished. We hypothesized that the resistance of apples to damage is associated with the biosynthesis of volatile esters and flavonoids. The results of this study bear substantial importance in facilitating the functional verification analysis of pivotal defense genes in 'Red Fuji' apple fruit.

2. Materials and methods

2.1. Fruit materials

The "Red Fuji" apple (*Malus* × *domestica* Borkh. Red Fuji) was purchased from a local store in Hangzhou, Zhejiang Province, China. The apples were selected based on their uniform size and color, commercial ripeness, absence of mechanical damage, and lack of signs of pest or disease. To prevent mechanical damage during transportation, the apples were packed in single-layer double corrugated boxes and covered with foam mesh bags. Upon arrival at the laboratory, the apples were carefully examined to exclude any that had been damaged during transport.

2.2. Impact damage treatment of apple fruit

To simulate the impact, the fruit was dropped from a height of 40 mm onto a marble floor. The fruit was immediately caught after the fall to prevent secondary damage. The fruits were stored at 20 °C after impact, and samples were collected on 0, 2, 6, 24, and 60 d of storage. At each time point, a total of 15 apple fruits are randomly sampled and subsequently divided into three biological replicates, where each replicate consists of 5 fruits. The damaged part and undamaged part of the fruit were identified as the impact group (ID) and control group (CK_{ID}), respectively. The flesh samples were finely chopped, quickly frozen in liquid nitrogen, and stored at −80 °C.

The experiment encompassed two distinct groups: the impact group (ID) and the control group (CK_{ID}). Samples were collected from both groups at five time points, enabling subsequent analysis of metabolites and transcriptomes. The analysis comprised the identification and examination of metabolites and transcriptomes individually, as well as a comprehensive joint analysis of transcriptomes and key metabolites. The metabolite data analysis incorporated principal component analysis (PCA), cluster analysis, and assessment of replicate correlation. The transcriptome data analysis encompassed sequence alignment against a specified reference genome, differential expression analysis, functional annotation of genes exhibiting differential expression, and functional enrichment analysis based on expression levels. The joint analysis entailed correlation analysis and the investigation of eight KEGG pathways.

2.3. Detection and analysis of transcriptome

2.3.1. Extraction of RNA

The total RNA extraction method used in this study was based on Wu et al. (2022). The method involved adding 0.5 g of pulp sample powder to 4 mL of pre-warmed CTAB/β-mercaptoethanol solution, followed by lysis and extraction using chloroform/isoamyl alcohol. The supernatant was then treated with lithium chloride, and the resulting precipitate was dissolved in SSTE and re-extracted with chloroform/isoamyl alcohol. The RNA was precipitated with ethanol, collected by centrifugation, and dissolved in DEPC water. The integrity and purity of the RNA samples were assessed by agarose gel electrophoresis and UV spectrophotometry.

2.3.2. Analysis of the transcriptome

RNA sequencing on fruit samples of impact and control groups at different storage times (0, 2 d, 6 d, 24 d and 60 d) was conducted using

the Illumina Hiseq sequencer platform (Beijing Biomarker Technologies Co., Ltd.). Each sampling point sample had three biological replicates. The data was preprocessed to remove low quality data and assembled with reference to the apple genome Malus × *domestica* Genome V1.0 database. GO enrichment analysis was performed using GOseq R package software, and KEGG signaling pathway enrichment analysis was performed using KOBAS software. Gene expression abundance was measured using the FPKM value (Fragments per kilobase of transcript per million fragments mapped), which was calculated as follows.

$$\mathrm{FPKM} = \frac{\text{cDNA Fragments}}{\text{Mapped Fragments (Millions)} \times \text{Transcript Length (kb)}}$$

2.4. Detection and analysis of a wide range of targeted metabolomes

2.4.1. Sample preparation and extraction

Fruit samples of impact and control groups at 6 d of storage were chosen for extensive targeted metabolomic assays conducted by Wuhan Metwell Biotechnology Co., Ltd. The pulp samples were first vacuum freeze-dried and ground to powder using a grinder. Then, 100 mg of the sample powder was dissolved in 0.6 mL of 70% methanol aqueous solution and left to extract overnight at 4 °C. The following day, the samples were centrifuged, and the supernatant was filtered and aspirated for UPLC-MS/MS analysis. Three biological replicates were conducted for each sampling point sample.

2.4.2. Conditions for ultra-performance liquid chromatography and tandem mass spectrometry

The primary method of data acquisition was through ultra-performance liquid chromatography (UPLC) and tandem mass spectrometry MS/MS. The liquid chromatography conditions and the mass spectrometry conditions were referred to Yang et al. (2022).

2.5. Statistical analysis

In order to understand the overall metabolic differences between sample groups and the variability within each group, PCA was employed. The data processing steps associated with PCA involve compressing the original data into a set of n principal components, thereby capturing the salient characteristics of the initial dataset. Principal Component 1 (PC1) denotes the most prominent feature within the multidimensional data matrix, followed by PC2, which represents the subsequent significant feature after PC1. This sequential pattern continues with PC3…PCn. The R software's built-in statistical function prcomp was used to conduct PCA (https://www.r-project.org).

To identify differential metabolites, the metabolomic data was subjected to analysis using Orthogonal Partial Least Squares-Discriminant Analysis (OPLS-DA). This technique employs predictive parameters such as R^2X, R^2Y, and Q^2 to assess the model's performance. R^2X represents the percentage of variance explained by the model for the independent variable matrix X, while R^2Y represents the percentage of variance explained for the dependent variable matrix Y. Q^2 is a measure of the model's predictive ability. The closer these three indicators are to 1, the more stable and reliable the model is considered. A Q^2 value greater than 0.5 is typically indicative of an effective model, while a Q^2 value exceeding 0.9 suggests an outstanding model. In the present study, Q^2 is 0.932, which proves the stable reliability of the model.

In addition to PCA, the ComplexHeatmap toolkit in R software was utilized to create cluster heat maps, radar plots, and Pearson correlation coefficients for clustering analysis and correlation analyses. Origin Pro 2020 Learning Edition software (OriginLab Corp., Northampton, MA) was used to generate histograms and differential metabolite classification heatmaps. For significance analysis, one-way analysis of variance (ANOVA) was performed using the SPSS 17.0 software package (IBM, New York, NY), and significant differences were indicated as $^*p < 0.05$, $^{**}p < 0.01$, and $^{***}p < 0.001$.

3. Results

3.1. Effect of impact damage on the transcriptome of apple fruit

3.1.1. Sequencing data and the quality of the data

RNA-Seq technology was employed to perform transcriptome analysis on 30 apple samples. A clean data set of 220.50 Gb was obtained, with each sample reaching 5.69 Gb and Q30 base percentage exceeding 94.23%. Alignment efficiency with the designated reference genome ranged from 66.41% to 71.96% for each sample. The sequencing quality of the impact-damaged apple transcriptome was statistically analyzed, and the results are presented in Table S1.

PCA was executed on the transcriptome data to examine the variations between samples, and the outcomes are demonstrated in Fig. 1a. The first two principal components, Principal Component 1 (PC1) and Principal Component 2 (PC2), could account for 62.3% and 18.7% of the total variance, respectively. At the PC1 level, d6 CK_{ID} could be distinguished from d6 ID distinctly. At the PC2 level, d2 CK_{ID} was evidently separable from d2 ID, and d6 CK_{ID} from d6 ID, while the distinction between the impact and control groups was less conspicuous at other storage times. These findings suggest that the transcriptomes of the diverse apple fruit samples were indistinguishable on the day after impact damage and could only be distinguished at 2 d and 6 d of storage, whereas the distinction was less prominent at 24 d and 60 d of storage.

3.1.2. Screening and expression analysis of differentially expressed genes (DEGs)

Table S2 shows the statistics of the impact damage on the number of DEGs in apple fruit during storage. The number of DEGs gradually decreased over time after the fruits were subjected to impact damage, with 2723 DEGs identified at 0 d, 2681 and 2189 DEGs identified at 2 d and 6 d, and 685 and 598 DEGs identified at 24 d and 60 d, respectively.

The Wayne diagram depicting the DEGs of apple fruit following impact damage during storage is exhibited in Fig. 1b. Amongst all the DEGs, a total of 124 were found to be common at each storage time point for both the impact and control groups. Notably, KEGG annotation of these DEGs revealed their association with various metabolic pathways, including flavonoid synthesis and phenylpropanoid biosynthesis pathways (10 genes), signal transduction pathway (9 genes), carbohydrate metabolism pathway (8 genes), transcription pathway (5 genes), amino acid and other amino acid metabolism pathways (5 genes), terpenoid and polyketide metabolism pathways (4 genes), and lipid metabolism pathways (3 genes), as well as environmental adaptation (3 genes), transport and catabolic pathways (3 genes), cofactor and vitamin metabolism pathways (2 genes), folding, sorting, and degradation pathways (2 genes), translation pathways (1 gene), and membrane transport pathways (1 gene).

3.1.3. Functional annotation of differentially expressed genes

The functional annotation of differentially expressed genes (DEGs) was performed using eight databases, and the results are presented in Table S3. At 0 d, 2 d, 6 d, 24 d, and 60 d of storage, a total of 2609, 2531, 2099, 670, and 581 DEGs, respectively, were annotated in the eight databases for both the impact and control groups of apple fruit.

3.1.4. GO functional annotation and enrichment analysis of DEGs

GO annotation and enrichment analysis of DEGs (depicted in Fig. 1c, 1e, 1 g, 1i, 1 k) were conducted to explore the biological processes associated with DEGs in both impact and control fruits. Specifically, at 0 d, DEGs between the impact and control groups were predominantly enriched in defense response, response to biotic stimulus, and response to oxygen-containing compound processes. At 2 d, DEGs were primarily enriched in translation and defense response processes. At 6 d, DEGs were enriched in cell wall organization and defense response processes. At 24 d, DEGs were chiefly enriched in cell wall organization and

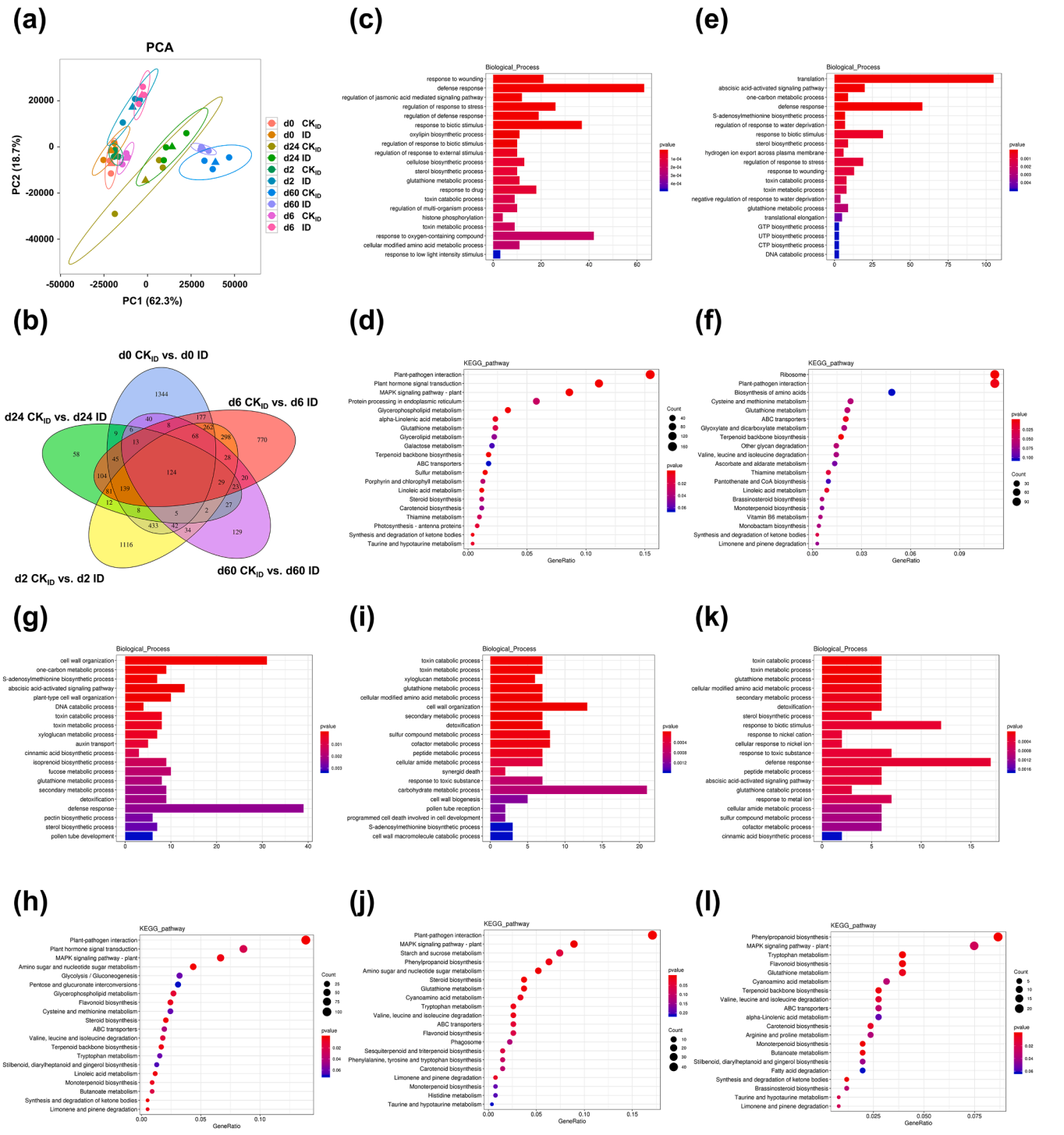

Fig. 1. Effect of impact damage on the transcriptome of apple fruit. PCA analysis of transcriptome data in ID and CK_{ID} group apples during storage. (b) Venn diagrams of DEGs in ID and CK_{ID} group apples during storage. (c, e, g, i, k) Biological Process of GO enrichment of DEGs in ID and CK_{ID} group apples on 0 d (c), 2 d (e), 6 d (g), 24 d (i), and 60 d (k) of storage. (d, f, h, j, l) KEGG enrichment of DEGs in ID and CK_{ID} group apples on 0 d (d), 2 d (f), 6 d (h), 24 d (j), and 60 d (l) of storage. ID: Impact damage; CK_{ID}: Control check for ID.

carbohydrate metabolism processes. Lastly, at 60 d, DEGs were mainly enriched in response to oxygen-containing compound and defense response process.

3.1.5. *Functional annotation and enrichment analysis of KEGG of DEGs*

The top 20 enriched metabolic pathways were identified by performing KEGG functional annotation and enrichment analysis of DEGs, as shown in Fig. 1d, 1f, 1 h, 1j, and 1 L. At day 0, metabolic pathways, such as plant-pathogen interaction, MAPK pathway-plant, and plant hormone signaling, exhibited the highest enrichment of DEGs between the impact and control groups. At 2 d, the majority of the DEGs were accumulated in metabolic pathways, such as ribosome, plant-pathogen interaction, and amino acid biosynthesis. At 6 d, the DEGs were mainly concentrated in metabolic pathways associated with amino sugar and nucleotide sugar metabolism, plant-pathogen interaction, MAPK pathway-plant, plant hormone signal transduction, and other

metabolic pathways. At 24 d, the DEGs were mainly concentrated in pathways involved in plant-pathogen interaction, MAPK signaling pathway-plant, and sucrose and starch metabolism. At 60 d, the DEGs were mostly concentrated in metabolic pathways, such as glutathione metabolism, tryptophan metabolism, flavonoid biosynthesis, and phenylpropanoid biosynthesis.

3.2. Effect of impact damage on the metabolome of apple fruit

3.2.1. PCA analysis and repeat correlation assessment

The variability between the impact and control group samples was evaluated using PCA analysis. As shown in Fig. 2a, PC1 and PC2 cumulatively contributed 18.44% and 47.40% of the variation, respectively. By using PCA analysis, the apple fruits in the impact and control groups could be easily distinguished.

For the biological replicates of the fruit samples, correlations were assessed using Pearson correlation coefficients (Fig. 2b). According to the results, there was a significant degree of data consistency among the three biological replicates of the impact and control groups, and the correlation coefficients of the samples within groups were higher than those between groups, indicating a high degree of data reliability.

3.2.2. Screening of differentially expressed metabolites (DEMs)

Based on broadly targeted metabolomic analysis methods, a total of 683 metabolites were identified in apple fruit samples. Of these, 175 metabolites, including 142 up-regulated and 33 down-regulated metabolites, were significantly altered after impact damage. Table S4 shows the details of DEMs. To further illustrate the patterns and expression levels of metabolite changes between the impact and control groups, the 175 DEMs were applied to a volcano plot analysis (Fig. 2c).

3.2.3. Classification of DEMs

The fold differences of DEMs between the impact and control groups of apple fruit were subjected to Log_2 transformation and subsequently plotted categorically in Fig. 2d. The identified metabolites were classified into various groups including 34 terpenoids, 30 flavonoids, 22 lipids, 17 amino acids and its derivatives, 15 phenolic acids, 12 nucleotides and its derivatives, 10 alkaloids, 10 others, 9 organic acids, 9 lignans and coumarins, and 7 tannin metabolites.

The top 10 metabolites with the largest fold difference were presented as bars in Fig. 2e. Among them, the up-regulated metabolites were isothankunic acid, 2,4,2′,4′-tetrahydroxy-3′-prenylchalcone, 11-keto-ursolic acid, succinic anhydride, Trans-5-O-(p-coumaroyl) shikimate, 2α,3α-epoxy-5,7,3′,4′-tetrahydroxyflavan-(4β-8-catechin), Procyanidin A2, S-allyl-L-cysteine, syringic acid, 1-oxo-siaresinolic acid. Downregulated metabolites were L-tryptophan, 1-methoxyindole-3-acetamide, methoxyindoleacetic acid, L-lysine, L-glutamine, 6-methylmercaptopurine, L-phenylalanine, N-benzylmethylene-isomethylamine, piceatannol-3′-O-glucoside, N-monomethyl-L-arginine.

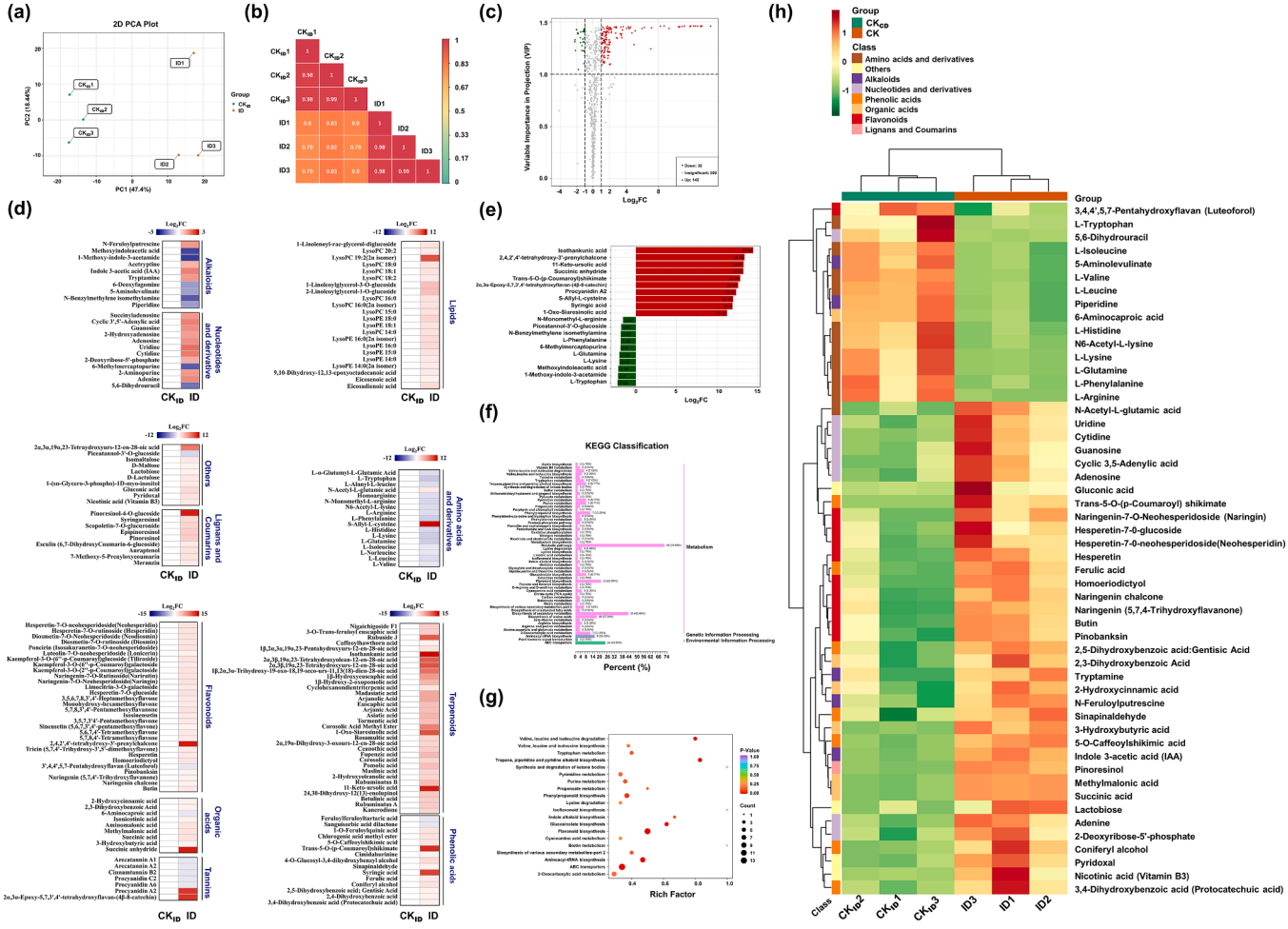

Fig. 2. Effect of impact damage on the metabolome of apple fruit. (a) PCA score plot metabolite profiles from CK_{ID} and ID group. (b) Correlation heat map of CK_{ID} and ID group. (c) Volcano plots of DEMs between CK_{ID} and ID group. (d) Classification of DEMs between CK_{ID} and ID group. (e) Bar Chart of DEMs between CK_{ID} and ID group (Top 10). (f) KEGG classification of DEMs between CK_{ID} and ID group. (g) KEGG enrichment of DEMs between CK_{ID} and ID group. (h) KEGG heatmap of DEMs between CK_{ID} and ID group. ID: Impact damage; CK_{ID}: Control check for ID.

3.2.4. Functional annotation and enrichment analysis of the KEGG metabolic pathway for DEMs

The 175 DEMs between apple fruit samples of the impact and control groups were annotated with KEGG pathways, and the KEGG classification (Fig. 2f) and KEGG enrichment analysis (Fig. 2g) were plotted. The first 20 enriched pathways mainly included (1) metabolic pathways related to biosynthesis of other secondary metabolites, such as flavonoid biosynthesis, phenylpropane biosynthesis, isoflavonoid biosynthesis, indole alkaloid biosynthesis, tropane, piperidine and pyridine alkaloid biosynthesis, stilbenoid, diarylheptanoid and gingerol biosynthesis, glucosinolate biosynthesis, etc. (2) metabolic pathways related to amino acid metabolism, such as valine, leucine and isoleucine biosynthesis, valine, leucine and isoleucine catabolism, tryptophan metabolism, lysine catabolism, etc. (3) metabolic pathways related to the metabolism of other amino acids, such as cyanoamino acid metabolism; (4) metabolic pathways related to nucleotide metabolism, such as purine metabolism, pyrimidine metabolism, etc.; (5) metabolic pathways related to carbohydrate metabolism, such as propanoate metabolism; (6) metabolic pathways related to global and outline maps, such as 2-oxocarboxylic acid metabolism; (7) metabolic pathways related to cofactor and vitamin metabolism, such as biotin metabolism (8) metabolic pathways related to membrane transport, such as ABC transport; (9) metabolic pathways related to translation, such as aminoacyl-tRNA biosynthesis; (10) metabolic pathways related to lipid metabolism, such as ketone synthesis and degradation. In addition, the KEGG enrichment map results showed that six metabolic pathways were significantly enriched (p-value < 0.05), including flavonoid biosynthesis, tropane, piperidine and pyridine alkaloid biosynthesis, aminoacyl-tRNA biosynthesis, valine, leucine and isoleucine degradation, thioglucoside biosynthesis and ABC transport.

3.2.5. Clustering analysis of KEGG annotation information of DEMs

To analyze the modifications in the content of DEMs within potentially significant metabolic pathways in both the impact and control groups, KEGG pathways that contained no less than five distinct differential metabolites were selected based on the DEMs' annotation information within the KEGG pathway, and all the differential metabolites annotated to these pathways underwent cluster analysis (as depicted in Fig. 2h). The results revealed that the aforementioned DEMs consisted of eleven amino acids and their derivatives, ten flavonoid metabolites, eight nucleotides and their derivatives, seven phenolic acid metabolites, six organic acid metabolites, five alkaloid metabolites, four additional categories of metabolites, as well as one lignan and coumarin metabolite.

3.3. Integrating transcriptome and metabolome analysis of apple fruit under impact damage

3.3.1. Correlation analysis of transcriptome and metabolome expression data

To demonstrate the correlation of DEGs and DEMs, a nine-quadrant plot was used to analyze the differential multiplicity of DEGs and DEMs with Pearson correlation coefficients greater than 0.8 (Fig. 3a). The analysis revealed that genes and metabolites in quadrants 3 and 7 had similar patterns of differential expression, suggesting that genes positively regulate the expression of these metabolites. Further analysis showed that 2217 differential genes positively regulated 190 differential metabolites, which may be associated with the response of apple fruit to impact damage. On the other hand, the opposite patterns of differential expression for genes and metabolites in quadrants 1 and 9 suggest that changes in the expression of these metabolites may be negatively regulated by genes. The analysis showed that 2184 differential genes adversely regulated 188 differential metabolites, which may also be related to how apple fruit responds to impact damage as a source of stress. When genes or metabolites were up- or down-regulated but not both, they were located in quadrants 2, 4, 6, and 8. Quadrant 5 indicates no differential expression of both genes and metabolites.

3.3.2. Analysis of the KEGG pathway for co-enrichment of DEGs and DEMs

Enrichment analysis was performed on the DEGs and DEMs between fruit samples from the impact and control groups, and the enrichment levels of metabolic pathways with both DEGs and DEMs were shown in Fig. 3b. The results showed significant enrichment (p-value < 0.05) of DEGs or DEMs annotated in the flavonoid biosynthesis, degradation of valine, leucine, and isoleucine, ABC transport, linoleic acid metabolism, ketone body synthesis and degradation, plant hormone signal transduction, and butanoate metabolism pathways. Among them, only the flavonoid biosynthesis, ABC transport, and degradation of valine, leucine, and isoleucine pathways showed significant enrichment of both DEGs and DEMs (p-value < 0.05).

3.3.3. Analysis of differential gene and differential metabolite expression in the flavonoid biosynthesis pathway

As shown in Fig. 4a, 19 DEGs and 12 DEMs were annotated in the flavonoid biosynthesis pathway. Nineteen DEGs and twelve DEMs in the flavonoid biosynthesis pathway were annotated to observe their expression changes between the impact and control groups of apple fruits, as shown in Fig. 3c (i). Among the 19 DEGs, *MdCHI* (Chalcone–flavonone isomerase, *MDP0000759336*, *MDP0000682951*, *MDP0000274127*), *MdF3H* (Naringenin, 2-oxoglutarate 3-dioxygenase, *newGene 4095*), *MdCCoAOMT* (*MDP0000226279*), *MdUGT88A1* (UDP-glycosyltransferase 88A1, *MDP0000294531*), *MdCYP450 98A2* (*MDP0000836708*, *MDP0000466557*, *MDP0000287029*), *MdCYP75B2* (Flavonoid 3′-monooxygenase, *MDP0000190489*), *MdPKS5* (Polyketide synthase 5, *MDP0000686661*), *MdBAHD1* (BAHD acyltransferase At5g47980, *MDP0000641254*), *MdSALAT* (Salutaridinol 7-O-acetyltransferase, *MDP0000391122*), *MdHST* (Shikimate O-hydroxycinnamoyltransferase, *MDP0000307780*, *MDP0000264424*), *MdTAT* (Tabersonine-19-hydroxy-O-acetyltransferase, *MDP0000271527*), and *MdLAR* (Leucoanthocyanidin reductase, *newGene 2561*) were significantly upregulated after being mechanically damaged by impact. *MdCER2* (Protein ECERIFERUM 2, *MDP0000275850*) and *MdVSR7* (Vacuolar-sorting receptor 7, *MDP0000242900*) were significantly downregulated after impact. The information for 12 DEMs is shown in Fig. 3c (ii), among which, *trans*-5-O-caffeoylquinic acid content increased significantly ($Log_2FC = 12.84$) after being mechanically damaged by impact.

Correlation analysis was performed on DEGs and DEMs in the flavonoid biosynthesis pathway with Pearson correlation coefficients greater than 0.8. The correlation coefficients between the DEGs and DEMs are shown in Table S4. Notably, 5-O-caffeoylquinate, *trans*-5-O-p-coumaroylshikimic acid, and naringin were significantly correlated with most of the DEGs.

3.3.4. Analysis of differential gene and differential metabolite expression in the ABC transporters pathway

As shown in Fig. S1, 15 DEGs and 14 DEMs were annotated in the ABC transport pathway. Fifteen DEGs are shown in Fig. 3d (i). Among them, *MdABCB1* (ABC transporter B family member 1, *MDP0000183294*), *MdABCB11* (ABC transporter B family member 11, *MDP0000302716*, *MDP0000849544*), *MdABCB19* (ABC transporter B family member 19, *MDP0000248803*), *MdABCC3* (ABC transporter C family member 3, *MDP0000842997*), *MdABCC4* (ABC transporter C family member 4, *MDP0000211981*, *MDP0000321920*), *MdABCC5* (ABC transporter C family member 5, *MDP0000269936*), *MdABCC10* (ABC transporter C family member 10, *MDP0000842161*), *MdABCC14* (ABC transporter C family member 14, *MDP0000138090*), *MdABCG3* (ABC transporter G family member 3, *MDP0000942052*), *MdABCG36* (ABC transporter G family member 36, *newGene 9561*), *MdPDR1* (Pleiotropic drug resistance protein 1, *newGene 755*), *MdPDR2* (Pleiotropic drug resistance protein 2, *newGene 5084*), and other genes were significantly upregulated after being mechanically damaged by impact;

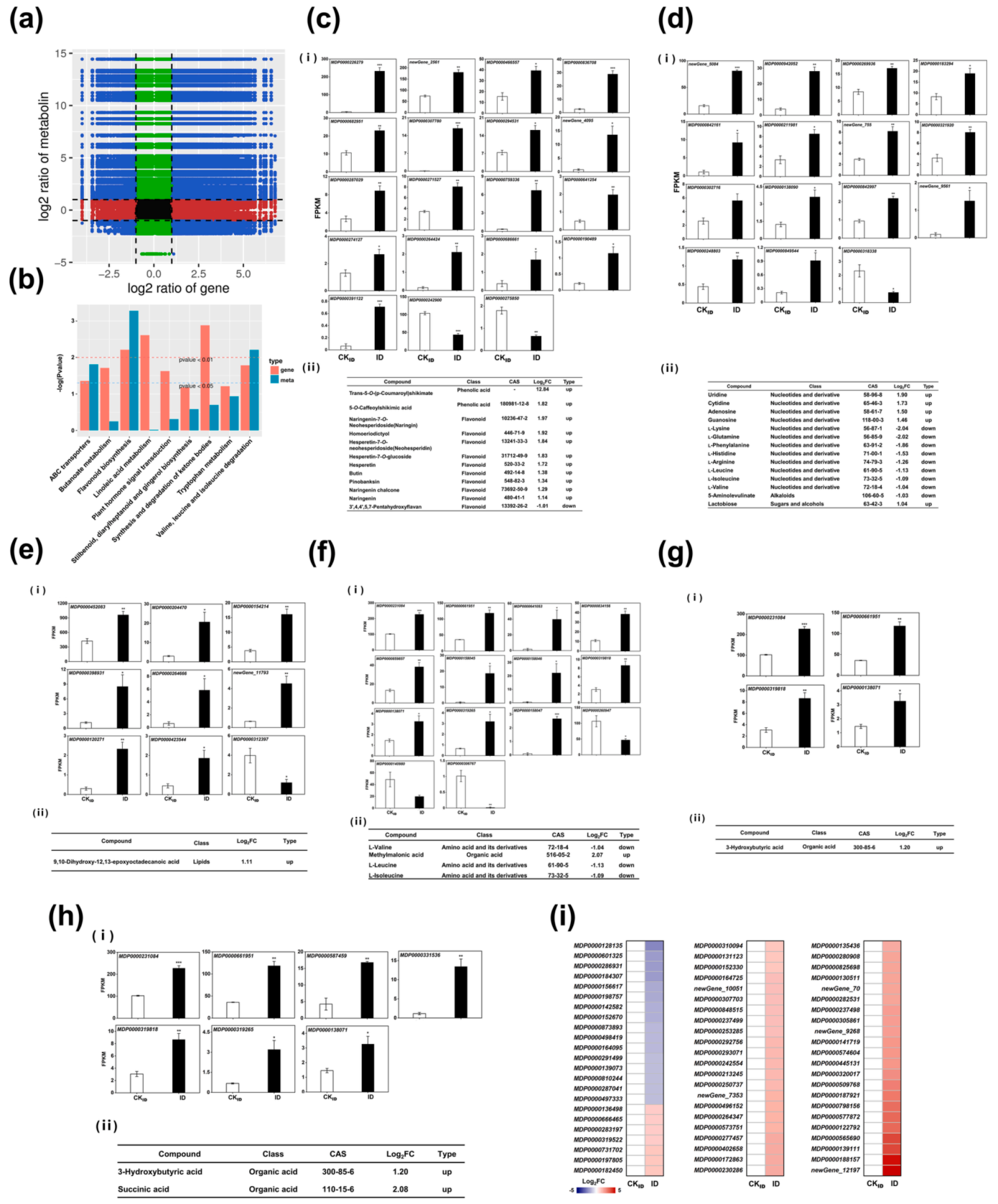

Fig. 3. Integrating transcriptome and metabolome analysis of apple fruit under impact damage. (a) Ninequadrants of DEMs and DEGs between CK_{ID} and ID group apples. The black dotted line, from left to right and top to bottom, is divided into quadrants 1–9 in order. (b) KEGG *P*-value of DEMs and DEGs between CK_{ID} and ID group apples. (c-i) Expression profiles of DEGs (i) and DEMs (ii) related to (c) flavonoid biosynthesis, (d) ABC transporters, (e) linoleic acid, (f) valine, leucine and isoleucine degradation, (g) synthesis and degradation of ketone bodies, (h) butanoate, (i) plant hormone signal transduction. ID: Impact damage; CK_{ID}: Control check for ID.

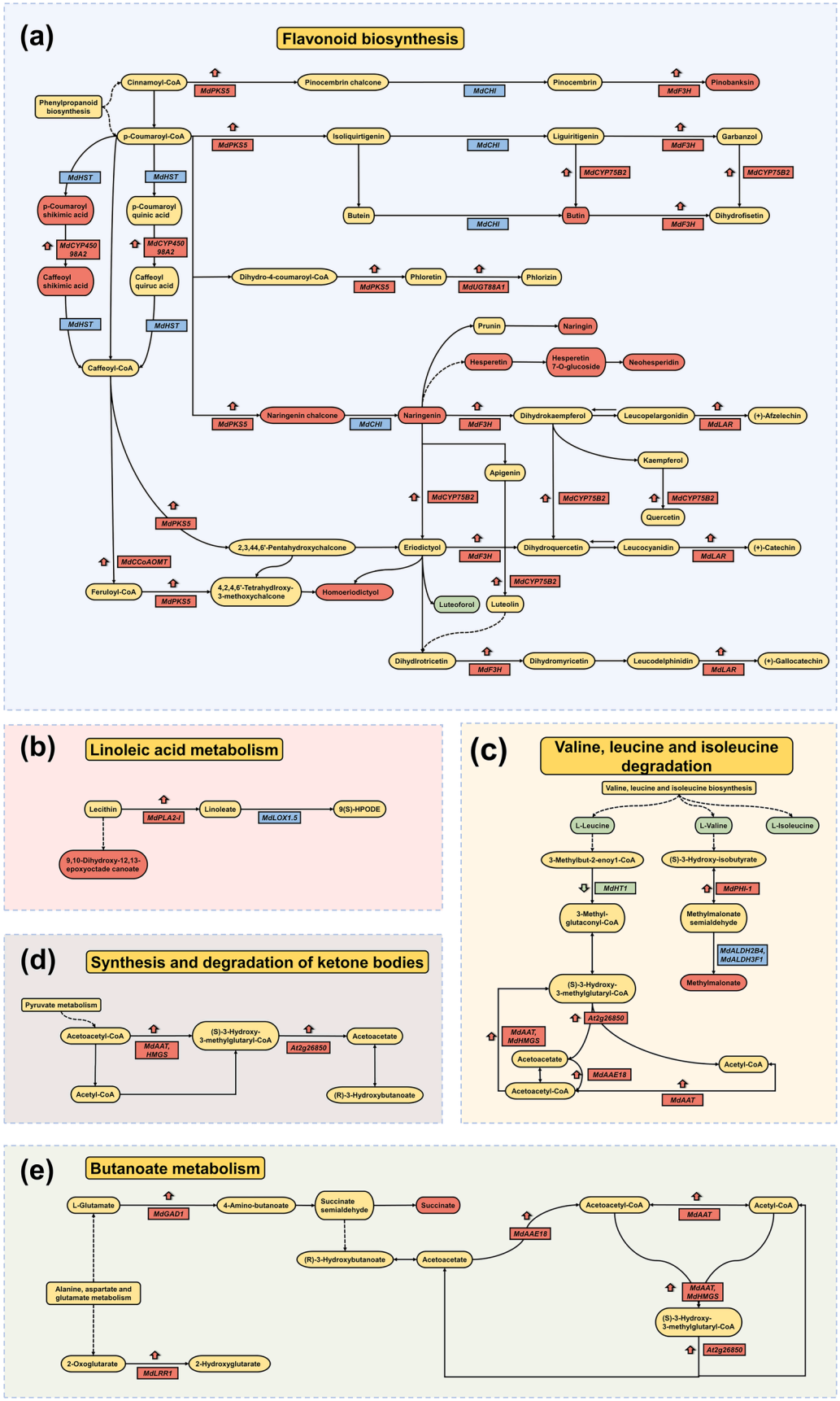

Fig. 4. Metabolic pathways for DEGs and DEMs of apples subjected to impact damage. (a) Flavonoid biosynthesis, (b) Linoleic acid, (c) Valine, leucine and isoleucine degradation, (d) Synthesis and degradation of ketone bodies, and (e) Butanoate metabolism. The red markers in the graph represent up-regulated DEGs/DEMs, the green markers represent down-regulated DEGs/DEMs, and the blue markers represent up-regulated/down-regulated DEGs/DEMs.

MdABCG22 (ABC transporter G family member 22, *MDP0000318338*) was significantly downregulated after being mechanically damaged by impact. Information on the 14 differentially expressed metabolites is shown in Fig. 3d (ii). Among them, the content of one alkaloid and eight amino acids and their derivatives decreased after being mechanically damaged by impact, while the content of one sugar and alcohol, four nucleotides, and their derivatives increased after being mechanically damaged by impact.

DEGs and DEMs with Pearson correlation coefficient greater than 0.8 in the ABC transport pathway were subjected to correlation analysis, and the correlation coefficients of DEGs and DEMs are shown in Table S5. Among them, *MdABCG3*, *MdABCC5*, *MdABCB19*, and *MdPDR2* were significantly correlated with most of the differential metabolites.

3.3.5. Analysis of differential gene and differential metabolite expression in the linoleic acid metabolism pathway

As shown in Fig. 4b, 9 DEGs and 1 DEM were annotated in the linoleic acid metabolic pathway. Nine DEGs were shown in Fig. 3e (i). Among them, *MdLOX5* (Linoleate 9S-lipoxygenase 5, *MDP0000204470*), *MdLOX1.5* (Probable linoleate 9S-lipoxygenase 5, *MDP0000120271*, *MDP0000264666*, *MDP0000398931*, *MDP0000423544*, *MDP0000452083*, *newGene 11793*), and *MdPLA2-I* (Probable phospholipase A2 homolog 1, *MDP0000154214*) were significantly upregulated after impact mechanical damage. *MdLOX1.5* (*MDP0000312397*) was significantly downregulated after impact mechanical damage. One DEM is shown in Fig. 3e (ii), in which the content of 9,10-dihydroxy-12,13-epoxy-octadecanoic acid increased after impact mechanical damage.

Further correlation analysis of 9 DEGs and 1 DEM identified in the comparison between impact and control groups showed that 9,10-dihydroxy-12,13-epoxy-octadecanoic acid was significantly positively correlated with *MdPLA2-I* (0.977***) and *MdLOX1.5* (*newGene 11793*) (0.938***).

3.3.6. Analysis of differential gene and differential metabolite expression in the valine, leucine and isoleucine degradation pathway

As shown in Fig. 4c, 14 DEGs and 4 DEMs were annotated in the valine, leucine, and isoleucine degradation pathway. Fourteen DEGs were identified as shown in Fig. 3f (i), including *MdAAT*, *MdHMGS* (*MDP0000138071*, *MDP0000661951*), *MdALDH2B7* (Aldehyde dehydrogenase family 2 member B7, *MDP0000834156*, *MDP0000859857*), *MdPHI-1* (Protein PHOSPHATE-INDUCED 1, *MDP0000158045*, *MDP0000158046*, *MDP0000158047*), *MdAAE18* (Probable acyl-activating enzyme 18, peroxisomal, *MDP0000319265*), *At2g26850* (F-box protein At2g26850, *MDP0000319818*), *MdEXL2* (Protein EXORDIUM-like 2, *MDP0000641053*), which were significantly upregulated after experiencing mechanical damage caused by impact. In contrast, *MdHT1* (Serine/threonine/tyrosine-protein kinase HT1, *MDP0000306767*), MdALDH3F1 (Aldehyde dehydrogenase family 3 member F1, *MDP0000260947*), and *MdALDH2B4* (Aldehyde dehydrogenase family 2 member B4, *MDP0000140980*) were significantly downregulated after experiencing mechanical damage caused by impact. Information about the four DEMs is shown in Fig. 3f (ii), in which the content of methylmalonic acid increased after experiencing mechanical damage caused by impact, while the contents of L-valine, L-leucine, and L-isoleucine decreased after experiencing mechanical damage caused by impact.

A correlation analysis was conducted on the DEGs and DEMs with Pearson correlation coefficients greater than 0.8 for valine, leucine, and isoleucine biodegradation. The correlation coefficients of the DEGs and DEMs are shown in Table S6. L-valine, L-leucine, and L-isoleucine were significantly negatively correlated with most DEGs, while methylmalonic acid was significantly negatively correlated with most DEGs.

3.3.7. Analysis of differential gene and differential metabolite expression in ketone bodies synthesis and degradation pathway

As shown in Fig. 4d, four DEGs and one DEM were annotated on the ketone synthesis and degradation pathway. The expression levels of the four DEGs are shown in Fig. 3g (i). Among them, *MdAAT*, *HMGS* (*MDP0000138071*, *MDP0000661951*), and *At2g26850* (*MDP0000319818*) were significantly upregulated after experiencing mechanical damage caused by impact. Information about one DEM is shown in Fig. 3g (ii), in which the content of 3-hydroxybutyrate increased after experiencing mechanical damage caused by impact. Further correlation analysis of the four DEGs and one DEM revealed a significant positive correlation between 3-hydroxybutyrate and *MdAAT* (0.976***), *At2g26850* (0.920***), and *HMGS* (*MDP0000661951*) (0.967***).

3.3.8. Analysis of differential gene and differential metabolite expression in butanoate metabolism pathway

As shown in Fig. 4e, 7 DEGs and 2 DEMs were annotated in the butanoate metabolism pathway. The expression levels of the 7 DEGs are shown in Fig. 3h (i), and genes such as *MdAAT*, *MdHMGS* (*MDP0000138071*, *MDP0000661951*), *MdAAE18* (Probable acyl-activating enzyme 18, *MDP0000319265*), *At2g26850* (F-box protein At2g26850, *MDP0000319818*), *MdLRR1* (Leucine-rich repeat protein 1, *MDP0000331536*), *MdGAD1* (Glutamate decarboxylase 1, *MDP0000587459*) were significantly up-regulated after impact mechanical compression. Information on the 2 DEMs is shown in Fig. 3h (ii), where the contents of succinic acid and 3-hydroxybutyric acid increased after experiencing mechanical damage caused by impact. Further correlation analysis of the 7 DEGs and 2 DEMs revealed that succinic acid was significantly positively correlated with *MdHMGS* (*MDP0000661951*) (0.983***), *MdLRR1* (0.935***), *At2g26850* (0.94***), *MdAAE18* (0.951***), and *MdAAT* (0.978***). 3-hydroxybutyric acid was significantly positively correlated with *MdHMGS* (*MDP0000661951*) (0.967***), *MdLRR1* (0.97***), *At2g26850* (0.92***), *MdAAE18* (0.931***), and *MdAAT* (0.976***).

3.3.9. Analysis of differential gene and differential metabolite expression in plant hormone signal transduction pathway

As shown in Figure S2, there were 67 annotated DEGs and 1 annotated DEM in the plant hormone signal transduction pathway. As shown in Fig. 3i, the 67 DEGs included 51 up-regulated genes and 16 down-regulated genes. Information on the 1 DEM is shown in Table S7, with an increase in the content of Indole 3-acetic acid (IAA) after impact damage. Further correlation analysis of the 67 DEGs and 1 DEM revealed that Indole-3-acetic acid was significantly correlated with 43 DEGs, as shown in Table S8.

4. Discussion

Flavonoid metabolism represents a significant branch of the phenylpropanoid pathway and has the potential to generate more than 6,000 polyphenolic metabolites (Hichri et al., 2011). Flavonoid compounds are classified into nine categories, namely chalcones, flavanones, flavones, isoflavones, dihydroflavonols, flavonols, anthocyanidins, anthocyanins, and aurones, based on the variation of the heterocyclic C ring (Nakayama et al., 2019). As effective antioxidants, flavonoid compounds have been shown to alleviate oxidative damage caused by non-biological stresses, such as soil salinity, drought, and extreme temperatures, through the accumulation of reactive oxygen species (Nakabayashi & Saito, 2015). Research has demonstrated that the upregulation of *F3H* and *DFR* genes in plants such as purple clover (Feyissa et al., 2019) and Arabidopsis thaliana (Nakabayashi et al., 2014) can enhance drought tolerance by synthesizing anthocyanins. Furthermore, cold stress has been shown to induce the upregulation of *CHS*, *CHI*, *FLS*, and *DFR* genes associated with flavonoid biosynthesis, thus promoting the accumulation of flavonoids and improving plant adaptability to low-temperature environments, as evidenced in chamomile (Zhang et al., 2019) and apples (An et al., 2020). In this study, we observed a significant upregulation of key genes in the flavonoid biosynthesis pathway, such as *MdCHI*, *MdF3H*, *MdCCoAOMT*, and

MdUGT88A1, in apple fruit subjected to impact damage. Furthermore, the concentration of flavonoid pathway metabolites, including *trans*-5-O-p-coumaroyl-mongolinoate, naringin, kaempferol 3-O-rutinoside, phloretin 2′-O-glucoside, luteolin 7-O-glucoside, and hesperetin chalcone, increased. Our findings suggest that apple fruit may activate a stress response mechanism to mitigate the effects of impact damage by promoting the accumulation of flavonoids.

The ABC transporter superfamily, ubiquitous in both eukaryotic and prokaryotic organisms, utilizes ATP hydrolysis to facilitate the transport of various biomolecules across membranes, such as amino acids, peptides, metal ions, cell metabolites, proteins, and sugars (Yazaki, 2006). With a crucial role in transporting endogenous secondary metabolites, encompassing phenols (Bartholomew et al., 2002), terpenoids (Jasiński et al., 2001), and alkaloids (Terasaka et al., 2005), ABC transporters are integral in the plant defense mechanism against fungal pathogens, by shuttling antimicrobial secondary metabolites to the periphery of host-pathogen interaction cells (Yazaki, 2006). In the present study, 13 ABC transporters were significantly upregulated in apple fruit after impact damage, which led to the increase of a multitude of secondary metabolites, such as lignins, tannins, coumarins, alkaloids, flavonoids, and terpenoids. Hence, it is postulated that ABC transporters could be involved in the transportation of secondary metabolites in response to impact damage in apple fruit.

Nine DEGs were identified in the linoleic acid metabolism pathway in apple fruit after being subjected to impact damage. Notably, *MdLOX5*, *MdPLA2-I*, and six *MdLOX1.5* (Probable *LOX5*) genes were significantly upregulated. Prior research has demonstrated that lipoxygenase (LOX) catalyzes the oxygenation of unsaturated fatty acids, leading to the generation of oxylipins through enzymatic or non-enzymatic pathways. These compounds participate in regulating plant growth, development, and stress responses. LOX gene expression is induced in response to various stresses, such as mechanical damage, drought, pathogen infection, and UV radiation (Grechkin, 1998). In beans, Mazur et al. (2018) discovered that mechanical damage induced the expression of *PcLOXA*, *PcLOXB*, and *PcLOXD*. Similarly, (Chauvin et al., 2013) observed that *AtLOX2*, *AtLOX3*, *AtLOX4*, and *AtLOX6* contribute to the rapid formation of jasmonic acid in mechanically damaged Arabidopsis leaves. LOX is the critical enzyme in the first catalytic step of volatile ester biosynthesis and plays a pivotal role in the synthesis of apple volatile compounds (Kumar et al., 2015). Furthermore, AAT, as the key enzyme in the final limiting step of volatile ester biosynthesis, also plays a significant role in fruit volatile compound synthesis (Cao et al., 2021; Yang et al., 2020). The present study identified metabolic pathways enriched with both DEGs and DEMs in apple fruit exposed to impact damage stress. Remarkably, *MdAAT* genes were significantly upregulated and annotated in pathways such as the degradation of valine, leucine, and isoleucine, ketone body synthesis and degradation, and butanoate metabolism. Consequently, it is speculated that apple fruit may promote the synthesis of volatile esters by inducing the expression of *MdLOX* and *MdAAT* genes in the LOX pathway in response to impact damage stress.

5. Conclusions

The present study conducted a hybrid analysis of the transcriptome and metabolome on apples subjected to mechanical damage. After being subjected to impact damage, the expression levels of 124 DEGs were consistently higher during storage, which enriched in biological processes related to defense response, response to biotic stimulus, translation, and cell wall organization. Additionally, the levels of several DEMs were significantly increased, including jasmonic acid, 2,4,2′,4′-tetrahydroxy-3′-pentenyl chalcone, 11-keto-ursolic acid, succinic anhydride, and *trans*-5-O-p-coumaroyl quinic acid, with all being upregulated. Metabolic pathway analysis showed that the annotated metabolic pathways of DEGs and DEMs included flavonoid biosynthesis, ABC transport, linoleic acid metabolism, ketone body synthesis and degradation, degradation of valine, leucine, and isoleucine, butanoate metabolism, and plant hormone signal transduction pathways (p-value < 0.05). Correlation analysis between transcriptome and metabolome data showed up-regulation of *MdAAT*, *MdLOX5*, and six *MdLOX1.5* genes in the LOX pathway, possibly related to biosynthesis of volatile esters in impact-damaged fruits. Up-regulation of key flavonoid synthesis genes, such as *MdCHI*, *MdF3H*, *MdCCoAOMT*, and *MdUGT88A1*, indicated flavonoid accumulation in response to mechanical damage stress. Upregulation of 13 ABC transporters and accumulation of secondary metabolites suggested their possible involvement in transporting secondary metabolites during mechanical damage stress. Overall, the results of the present study furnish additional biological insights into the metabolic networks and molecular mechanisms underlying the response of apple fruits to impact damage. These insights can potentially aid in the development of more efficacious strategies for minimizing impact damage and breeding fruit cultivars with heightened resistance to impact damage.

Funding

This work was supported by Key R&D Program of Shandong Province, China (2022TZXD0022) and Fundamental Research Funds for the Central Universities (2021FZZX001-55).

Ethical approval

This article does not contain any studies with human participants or animals performed by any of the authors.

Informed consent

Not applicable.

Declaration of Competing Interest

The authors declare that they have no known competing financial interests or personal relationships that could have appeared to influence the work reported in this paper.

Data availability

The authors do not have permission to share data.

Appendix A. Supplementary data

Supplementary data to this article can be found online at https://doi.org/10.1016/j.fochms.2023.100176.

References

Abanoz, Y. Y., & Okcu, Z. (2022). Biochemical content of cherry laurel (Prunus laurocerasus L.) fruits with edible coatings based on caseinat, Semperfresh and lecithin. *Turkish Journal of Agriculture and Forestry, 46*(6), 908–918. https://doi.org/10.55730/1300-011X.3052.

M.S. Afridi S. Ali A. Salam W. César Terra A. Hafeez A. Sumaira B., S. AlTami, M., Ameen, F., Ercisli, S., Marc, R. A., Medeiros, F. H. V., & Karunakaran, R. Plant Microbiome Engineering: Hopes or Hypes Biology 11 12 2022 1782 10.3390/biology11121782.

An, J., Wang, X., Zhang, X., Xu, H., Bi, S., You, C., & Hao, Y. (2020). An apple MYB transcription factor regulates cold tolerance and anthocyanin accumulation and undergoes MIEL1-mediated degradation. *Plant Biotechnology Journal, 18*(2), 337–353. https://doi.org/10.1111/pbi.13201

Bartholomew, D. M., Van Dyk, D. E., Lau, S.-M.-C., O'Keefe, D. P., Rea, P. A., & Viitanen, P. V. (2002). Alternate Energy-Dependent Pathways for the Vacuolar Uptake of Glucose and Glutathione Conjugates. *Plant Physiology, 130*(3), 1562–1572. https://doi.org/10.1104/pp.008334

Belay, Z. A., Caleb, O. J., Vorster, A., van Heerden, C., & Opara, U. L. (2020). Transcriptomic changes associated with husk scald incidence on pomegranate fruit peel during cold storage. *Food Research International, 135*, Article 109285. https://doi.org/10.1016/j.foodres.2020.109285

Bozhuyuk, M. R. (2022). Morphological and Biochemical Characterization of Wild Sour Cherry (Prunus cerasus L.). *Germplasm. Erwerbs-Obstbau, 64*(3), 357–363. https://doi.org/10.1007/s10341-022-00656-z

Cao, X., Wei, C., Duan, W., Gao, Y., Kuang, J., Liu, M., … Zhang, B. (2021). Transcriptional and epigenetic analysis reveals that NAC transcription factors regulate fruit flavor ester biosynthesis. *The Plant Journal, 106*(3), 785–800. https://doi.org/10.1111/tpj.15200

Chauvin, A., Caldelari, D., Wolfender, J., & Farmer, E. E. (2013). Four 13-lipoxygenases contribute to rapid jasmonate synthesis in wounded Arabidopsis thaliana leaves: A role for lipoxygenase 6 in responses to long-distance wound signals. *New Phytologist, 197*(2), 566–575. https://doi.org/10.1111/nph.12029

Dawadi, P., SHRESTHA, R., MISHRA, S., BISTA, S., RAUT, J. K., JOSHI, T. P., & BHATT, L. R. (2022). Nutritional value and antioxidant properties of Viburnum mullaha Buch.-Ham. ex D. Don fruit from central Nepal. *Turkish Journal of Agriculture and Forestry*, *46*(5), 781–789. https://doi.org/10.55730/1300-011X.3041.

Feyissa, B. A., Arshad, M., Gruber, M. Y., Kohalmi, S. E., & Hannoufa, A. (2019). The interplay between miR156/SPL13 and DFR/WD40–1 regulate drought tolerance in alfalfa. *BMC Plant Biology, 19*(1), 434. https://doi.org/10.1186/s12870-019-2059-5

Gong, R. G., Lai, J., Yang, W., Liao, M. A., Wang, Z. H., & Liang, G. L. (2015). Analysis of alterations to the transcriptome of Loquat (Eriobotrya japonica Lindl.) under low temperature stress via de novo sequencing. *Genetics and Molecular Research, 14*(3), 9423–9436. https://doi.org/10.4238/2015.August.14.6

Grechkin, A. (1998). Recent developments in biochemistry of the plant lipoxygenase pathway. *Progress in Lipid Research, 37*(5), 317–352. https://doi.org/10.1016/S0163-7827(98)00014-9

Hichri, I., Barrieu, F., Bogs, J., Kappel, C., Delrot, S., & Lauvergeat, V. (2011). Recent advances in the transcriptional regulation of the flavonoid biosynthetic pathway. *Journal of Experimental Botany, 62*(8), 2465–2483. https://doi.org/10.1093/jxb/erq442

Jasiński, M., Stukkens, Y., Degand, H., Purnelle, B., Marchand-Brynaert, J., & Boutry, M. (2001). A Plant Plasma Membrane ATP Binding Cassette-Type Transporter Is Involved in Antifungal Terpenoid Secretion. *The Plant Cell, 13*(5), 1095–1107. https://doi.org/10.1105/tpc.13.5.1095

Kumar, S., Rowan, D., Hunt, M., Chagné, D., Whitworth, C., & Souleyre, E. (2015). Genome-wide scans reveal genetic architecture of apple flavour volatiles. *Molecular Breeding, 35*(5). https://doi.org/10.1007/s11032-015-0312-7

Lin, M., Chen, J., Wu, D., & Chen, K. (2021). Volatile Profile and Biosynthesis of Post-harvest Apples are Affected by the Mechanical Damage. *Journal of Agricultural and Food Chemistry, 69*(33), 9716–9724. https://doi.org/10.1021/acs.jafc.1c03532

Lin, M., Fawole, O. A., Saeys, W., Wu, D., Wang, J., Opara, U. L., … Chen, K. (2022). Mechanical damages and packaging methods along the fresh fruit supply chain: A review. *Critical Reviews in Food Science and Nutrition, 1–20*. https://doi.org/10.1080/10408398.2022.2078783

Lin, S., Zeng, S., A, B., Yang, X., Yang, T., Zheng, G., Mao, G., & Wang, Y. (2021). Integrative Analysis of Transcriptome and Metabolome Reveals Salt Stress Orchestrating the Accumulation of Specialized Metabolites in Lycium barbarum L. Fruit. *International Journal of Molecular Sciences*, *22*(9), 4414. https://doi.org/10.3390/ijms22094414.

Liu, J., Zhang, X., & Sheng, J. (2022). Integrative analysis of the transcriptome and metabolome reveals the mechanism of saline–alkali stress tolerance in Astragalus membranaceus (Fisch) Bge. var. mongholicus (Bge.) Hsiao. *Food Quality and Safety, 6*. https://doi.org/10.1093/fqsafe/fyac001

Liu, X., Li, Y., Zhu, J., & Li, P. (2023). Integrative analysis of transcriptome reveals the possible mechanism of delayed leaf senescence in pak choi (Brassica rapa subsp. chinensis) following melatonin treatment. *Food Quality and Safety, 7*. https://doi.org/10.1093/fqsafe/fyac064

Mazur, R., Trzcinska-Danielewicz, J., Kozlowski, P., Kowalewska, Ł., Rumak, I., Shiell, B. J., … Garstka, M. (2018). Dark-chilling and subsequent photo-activation modulate expression and induce reversible association of chloroplast lipoxygenase with thylakoid membrane in runner bean (Phaseolus coccineus L.). *Plant Physiology and Biochemistry, 122*, 102–112. https://doi.org/10.1016/j.plaphy.2017.11.015

Moreno, A. S., Perotti, V. E., Margarit, E., Bello, F., Vázquez, D. E., Podestá, F. E., & Tripodi, K. E. J. (2018). Metabolic profiling and quality assessment during the postharvest of two tangor varieties subjected to heat treatments. *Postharvest Biology and Technology, 142*, 10–18. https://doi.org/10.1016/j.postharvbio.2018.03.014

Nakabayashi, R., & Saito, K. (2015). Integrated metabolomics for abiotic stress responses in plants. *Current Opinion in Plant Biology, 24*, 10–16. https://doi.org/10.1016/j.pbi.2015.01.003

Nakabayashi, R., Yonekura-Sakakibara, K., Urano, K., Suzuki, M., Yamada, Y., Nishizawa, T., … Saito, K. (2014). Enhancement of oxidative and drought tolerance in Arabidopsis by overaccumulation of antioxidant flavonoids. *The Plant Journal, 77*(3), 367–379. https://doi.org/10.1111/tpj.12388

Nakayama, T., Takahashi, S., & Waki, T. (2019). Formation of Flavonoid Metabolons: Functional Significance of Protein-Protein Interactions and Impact on Flavonoid Chemodiversity. *Frontiers in Plant Science, 10*. https://doi.org/10.3389/fpls.2019.00821

Pinu, F. R., Beale, D. J., Paten, A. M., Kouremenos, K., Swarup, S., Schirra, H. J., & Wishart, D. (2019). Systems Biology and Multi-Omics Integration: Viewpoints from the Metabolomics Research Community. *Metabolites, 9*(4), 76. https://doi.org/10.3390/metabo9040076

Rymbai, H., Verma, V. K., Talang, H., Assumi, S. R., Devi, M. B., Vanlalruati, Sangma, R. H. C., Biam, K. P., Chanu, L. J., Makdoh, B., Singh, A. R., Mawleiñ, J., Hazarika, S., & Mishra, V. K. (2023). Biochemical and antioxidant activity of wild edible fruits of the eastern Himalaya, India. *Frontiers in Nutrition*, *10*. https://doi.org/10.3389/fnut.2023.1039965.

Santin, M., Ranieri, A., Hauser, M.-T., Miras-Moreno, B., Rocchetti, G., Lucini, L., … Castagna, A. (2021). The outer influences the inner: Postharvest UV-B irradiation modulates peach flesh metabolome although shielded by the skin. *Food Chemistry, 338*, Article 127782. https://doi.org/10.1016/j.foodchem.2020.127782

Shen, C., Rao, J., Wu, Q., Wu, D., & Chen, K. (2021). The effect of indirect plasma-processed air pretreatment on the microbial loads, decay, and metabolites of Chinese bayberries. *LWT, 150*, Article 111998. https://doi.org/10.1016/j.lwt.2021.111998

Terasaka, K., Blakeslee, J. J., Titapiwatanakun, B., Peer, W. A., Bandyopadhyay, A., Makam, S. N., … Yazaki, K. (2005). PGP4, an ATP binding cassette P-glycoprotein, catalyzes auxin transport in Arabidopsis thaliana roots. *Plant Cell, 17*(11). https://doi.org/10.1105/tpc.105.035816

Tunsagool, P., Wang, X., Leelasuphakul, W., Jutidamrongphan, W., Phaonakrop, N., Jaresitthikunchai, J., … Li, L. (2019). Metabolomic study of stress responses leading to plant resistance in mandarin fruit mediated by preventive applications of Bacillus subtilis cyclic lipopeptides. *Postharvest Biology and Technology, 156*, Article 110946. https://doi.org/10.1016/j.postharvbio.2019.110946

Wu, Q., Shen, C., Li, J., Wu, D., & Chen, K. (2022). Application of indirect plasma-processed air on microbial inactivation and quality of yellow peaches during storage. *Innovative Food Science & Emerging Technologies, 79*, Article 103044. https://doi.org/10.1016/j.ifset.2022.103044

Yang, C., Duan, W., Xie, K., Ren, C., Zhu, C., Chen, K., & Zhang, B. (2020). Effect of salicylic acid treatment on sensory quality, flavor-related chemicals and gene expression in peach fruit after cold storage. *Postharvest Biology and Technology, 161*, Article 111089. https://doi.org/10.1016/j.postharvbio.2019.111089

Yang, Z., Wu, Q., Jiang, F., Zheng, D., Wu, D., & Chen, K. (2022). Indirect treatment of plasma-processed air to decrease decay and microbiota of strawberry fruit caused by mechanical damage. *Food Chemistry, 135225*. https://doi.org/10.1016/j.foodchem.2022.135225

Yazaki, K. (2006). ABC transporters involved in the transport of plant secondary metabolites. *FEBS Letters, 580*(4), 1183–1191. https://doi.org/10.1016/j.febslet.2005.12.009

Yun, Z., Qu, H., Wang, H., Zhu, F., Zhang, Z., Duan, X., … Jiang, Y. (2016). Comparative transcriptome and metabolome provides new insights into the regulatory mechanisms of accelerated senescence in litchi fruit after cold storage. *Scientific Reports, 6*(1), 19356. https://doi.org/10.1038/srep19356

Zhang, F., Ji, S., Wei, B., Cheng, S., Wang, Y., Hao, J., … Zhou, Q. (2020). Transcriptome analysis of postharvest blueberries (Vaccinium corymbosum 'Duke') in response to cold stress. *BMC Plant Biology, 20*(1), 80. https://doi.org/10.1186/s12870-020-2281-1

Zhang, M., Du, T., Yin, Y., Cao, H., Song, Z., Ye, M., … Wu, J. (2022). Synergistic effects of plant hormones on spontaneous late-ripening mutant of 'Jinghong' peach detected by transcriptome analysis. *Food Quality and Safety, 6*. https://doi.org/10.1093/fqsafe/fyac010

Zhang, Q., Zhai, J., Shao, L., Lin, W., & Peng, C. (2019). Accumulation of Anthocyanins: An Adaptation Strategy of Mikania micrantha to Low Temperature in Winter. *Frontiers in Plant Science, 10*. https://doi.org/10.3389/fpls.2019.01049

Zheng, Y., Liu, Z., Wang, H., Zhang, W., Li, S., & Xu, M. (2022). Transcriptome and genome analysis to identify C2H2 genes participating in low-temperature conditioning-alleviated postharvest chilling injury of peach fruit. *Food Quality and Safety, 6*. https://doi.org/10.1093/fqsafe/fyac059